Molecular Crystals and Liquid Crystals Science and Technology. Section A. Molecular Crystals and Liquid Crystals

Publication details, including instructions for authors and subscription information:
http://www.tandfonline.com/loi/gmcl19

Reorientation Dynamics of Liquid Crystal- Filled Porous Polymer Membranes

J. B. Whitehead Jr [a] & G. P. Crawford [b c]

[a] Depts of Physics and Astronomy & Chemistry and Biochemistry, University of Southern Mississippi, Hattiesburg, MS, 39406

[b] Liquid Crystal Institute, and Department of Physics, Kent State University, Kent, OH, 44242-0001

[c] Naval Research laboratory, Washington, D.C.

Version of record first published: 23 Sep 2006.

To cite this article: J. B. Whitehead Jr & G. P. Crawford (1995): Reorientation Dynamics of Liquid Crystal- Filled Porous Polymer Membranes, Molecular Crystals and Liquid Crystals Science and Technology. Section A. Molecular Crystals and Liquid Crystals, 262:1, 25-34

To link to this article: http://dx.doi.org/10.1080/10587259508033509

Mol. Cryst. Liq. Cryst. 1995, Vol. 262, pp. 25–34
Reprints available directly from the publisher
Photocopying permitted by license only

REORIENTATION DYNAMICS OF LIQUID CRYSTAL-FILLED POROUS POLYMER MEMBRANES

J.B. WHITEHEAD, JR.
Depts of Physics and Astronomy & Chemistry and Biochemistry
University of Southern Mississippi, Hattiesburg, MS 39406

G. P. CRAWFORD[a]
Liquid Crystal Institute and Department of Physics, Kent State University, Kent, OH 44242-0001

[a]Present address Naval Research laboratory, Washington, D.C.

Abstract When low-molecular weight liquid crystals are confined to small cylindrical volumes of porous polymer membranes, the elastic deformation energy and surface boundary effects play an increasing role as the surface-to-volume ratio is increased. For such materials confined to micron-sized volumes the free energy associated with the surface competes with the elastic deformation part of the free energy to determine the molecular organization or director configuration within the volume. An additional contribution to the free energy occurs when external fields are applied to such a system.

INTRODUCTION

In this study, polycarbonate membranes with cylindrically-shaped holes are permeated with a low-molecular weight nematic liquid crystal. The composite material is sandwiched between transparent conducting glass plates and laser light transmission is used to probe collective reorientation dynamics when the composite material is subjected to a 27 ms pulse (a.c. of 5 kHz) of varying amplitudes. Turn-on times and turn-off times are measured for cylinder diameters ranging from 0.1 to 1.0μm and voltage amplitudes up to 100 Vpp (peak-to-peak voltage).

The polycarbonate membrane/liquid crystal system is a model one to more easily study the effects of anchoring strength and confinement on the electrooptic

properties of liquid crystal polymer dispersions. Such dispersions are achieved by a number of phase separation methods.[1,2] This system is unique in that the dispersion is not the result of phase separation in which incomplete phase separation is problemmatic and the dispersed particles are less uniform in shape and size. The focus of this study is the electrooptic properties of polycarbonate membranes whose pre-formed cylindrical pores are filled with a low-molecular weight nematic liquid crystal.

Filtration membranes by Nuclepore Corporation are thin film polycarbonate disks which have cylindrical cavities whose axes are perpendicular to plane of the membrane. The cylindrical cavities are a result of an ion bombardment and a chemical etching process.[3] The diameters used in this study range from 0.1, 0.2, 0.4, 0.6, 0.8, and 1.0 μm. The membranes are filled a with K15 (5CB), a low-molecular nematic weight liquid crystal from EM Industries which has a nematic temperature range of 0^0 to 35^0 C.

Nematic ordering in confined geometries has been studied experimentally and theoretically by a number of researchers.[4,5,6,7,8] In confined geometries, such as micron and submicron droplets or cylindrical pores, the nematic structure is a result of competition between the bulk elastic, surface elastic, and external field contributions to the Frank elastic energy. Mathematically, the free energy is given by:

$$F=\frac{1}{2}\int_{vol}\left[K_{11}(\text{div }\mathbf{n})^2+K_{22}(\mathbf{n}\bullet\text{curl }\mathbf{n})^2+K_{33}(\mathbf{n}\times\text{curl }\mathbf{n})^2\right]dV$$
$$-\frac{1}{2}\int_{vol}K_{24}\text{div}(\mathbf{n}\times\text{curl }\mathbf{n}+\mathbf{n}\bullet\text{div }\mathbf{n})dV$$
$$-\frac{1}{2}\int_{\text{vol}}\Delta\varepsilon\varepsilon_0(\mathbf{E}\bullet\mathbf{n})^2dV+\frac{1}{2}\int_{surf}W_0\sin^2\phi dS \qquad \text{Eqn 1.}$$

where **n** is the nematic director (direction of the optic axis), K_{11}, K_{22}, and K_{33} are traditional splay, twist, and bend bulk elastic constants, respectively, K_{24} is often called the surface elastic constant because it enters in the free energy as a coefficient of the divergence of a volume integral which is readily transformed into a surface integral, $\Delta\varepsilon$

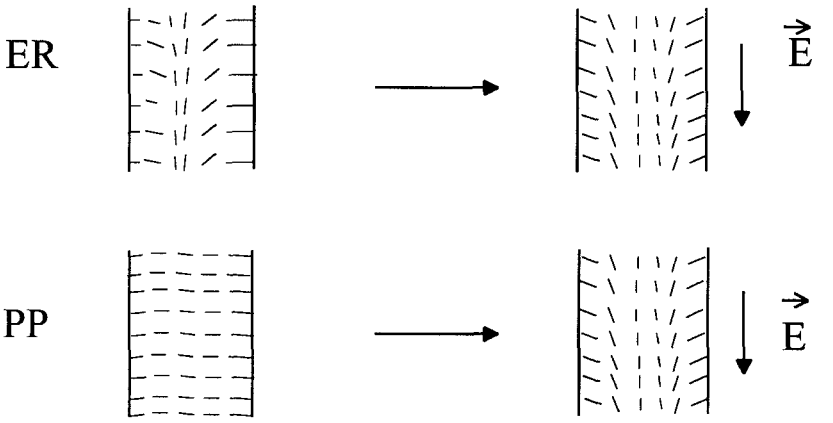

FIGURE 1 Model structures for the escaped-radial (ER) and planar-polar (PP) nematic sturctures with the expected qualitative behavior in an applied electric field.

is the dielectric anisotropy, W_o is the surface anchoring strength, and ϕ is the angle between the preferred homeotropic anchoring direction and the actual direction of the nematic director at the surface. Mathematically, the liquid crystal structure in a cylindrical pore is obtained using variational calculus to determine the solution(s) which minimizes the free energy of the system.

Numerous studies have focused on the structure of liquid crystals in cylindrical geometries. The two structures schematically illustrated in Figure 1 are known to occur in the cavities of Nuclepore membranes are the escaped-radial (ER) and the planar-polar (PP). [9,10,11] The ER structure, a splay-bend deformation, has homeotropic anchoring of the director at the cavity boundary and gradually escapes along the cylinder axis. The escaped-radial with point defects (ERPD) can also occur when defects are present along the cylinder axis since both directions of bend are energetically equivalent. [9] In the presence of an applied electric field parallel to the cylinder axis, we surmise that more directors will align along the cylinder axis. If an electric field is applied to the PP configuration, we expect this planar-splay-bend structure to experience a configuration transition to the ER configuration at a critical

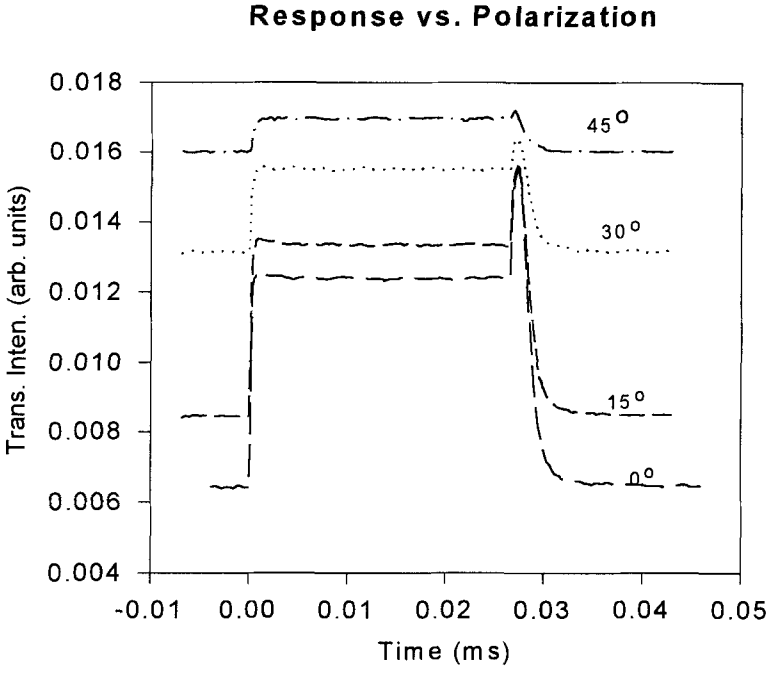

FIGURE 2 Response curves for a 1.0 μm diameter cylinder liquid crystal filled membrane for different incident polarizations for a V_{PP} = 10.0 V.

field, and then become more aligned along the cylinder axis as the field increases above the critical field (See Fig. 1).

EXPERIMENTAL

Samples are made by soaking the appropriate polycarbonate membrane in K15 to capillary fill the pores. This process is performed in the isotropic phase of K15 to enhance the filling process. After filling, the membrane is sandwiched between transparent conducting substrates.

The sample is subjected to an applied electric field by applying a sinusoidally varying voltage waveform to the substrates. The waveform is 26.6 ms in duration and the peak to peak voltage ranges from 0 to 100 Volts. The frequency of the sinusoidal region of the waveform is 5 kHz. A photodiode captures the light (λ= 632.8 nm)

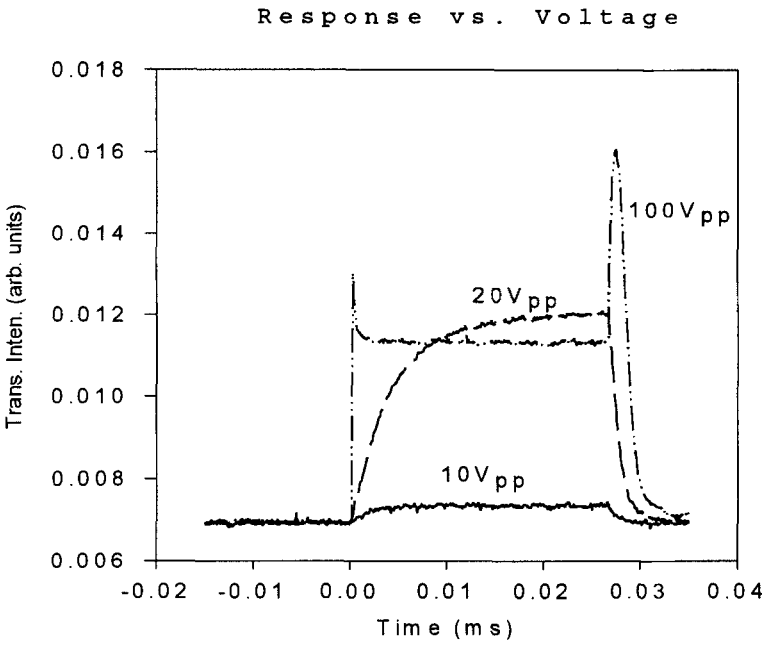

FIGURE 3 Response curves for a 1.0 μm diameter cylinder sample for 10, 20, and 100 volts peak-to-peak.

transmitted through the sample. The resulting electrical signal from the photodiode is fed into a digital oscilloscope which is triggered for acquisition at the onset of the voltage waveform.

The polycarbonate membrane is birefrengent; therefore, measurements are made with the incident light polarized so that the transmitted intensity is minimized for zero-applied voltage. In Figure 2, 0^0 corresponds to the polarization angle which yields the minimum transmission. The minimum and maximum transmitted intensities as well as their difference varies with incident polarization (see Fig. 2). The shape of the response is invariant to incident polarization. Therefore, the results are not biased by the choice of incident polarization. Therefore, each sample is measured with the incident polarization set at the minimum to maximize contrast and to enhance the signal-to-noise ration at low applied voltages. To further enhance the signal-to-noise ratio, the analyzed response curves are the result of sixteen voltage waveform

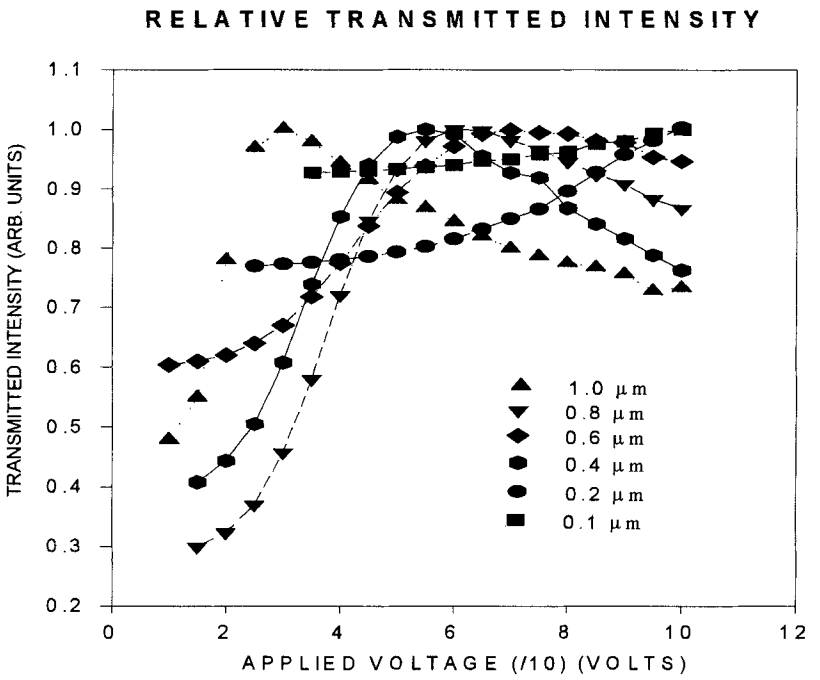

FIGURE 4 Normalized transmitted intensity for each cylinder diameter versus voltage.

applications which are averaged internally by the digital oscilloscope. A representative set of response curves is shown in Figure 3. The turn-on and turn-off times and the change in transmitted intensity are determined from the response curves such as the ones shown in Figure 3. The change in transmitted intensity is defined as:

$$<\Delta I>=<I_{on}> - <I_{off}> \qquad \text{Eqn. 2}$$

where $<I_{on}>$ is the average of the on-state transmission during application of the voltage pulse. $<I_{on}>$ is taken from the plateau area of the response curve. $<I_{off}>$ is the average transmitted intensity before the voltage pulse is applied. Figure 4 illustrates the voltage dependent normalized $<\Delta I>$ versus voltage for each cylinder size. A peak occurs above a "threshold voltage" at the instant applied voltage pulse ends (see Fig. 3).

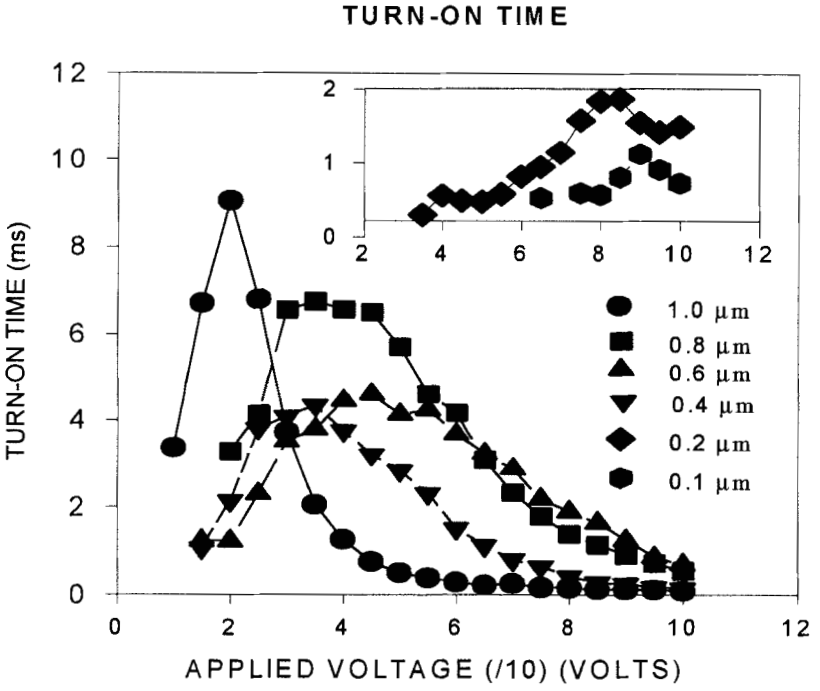

FIGURE 5 Turn-on times versus voltage for the various cylinder diameters.

This "threshold voltage" increases with decreasing cylinder size and is not present for the 0.1 and 0.2 μm cylinder sizes for the voltages in this study.

The turn-on and turn-off times are measured using the standard definitions. The turn-on time is defined as the time it takes for the transmitted intensity to rise from 10% to 90% of $\langle \Delta I \rangle$ at the onset of the voltage waveform and the turn-off time is the time it takes the transmitted intensity to decrease from 90% to 10% $\langle \Delta I \rangle$ at the end of the voltage waveform.

ANALYSIS

Figure 5 shows the voltage dependent turn-on time for the different cylinder sizes under investigation. From elastic deformation theory, one would expect the turn-on time to decrease with increasing voltage, but in this cylindrically defined geometry the

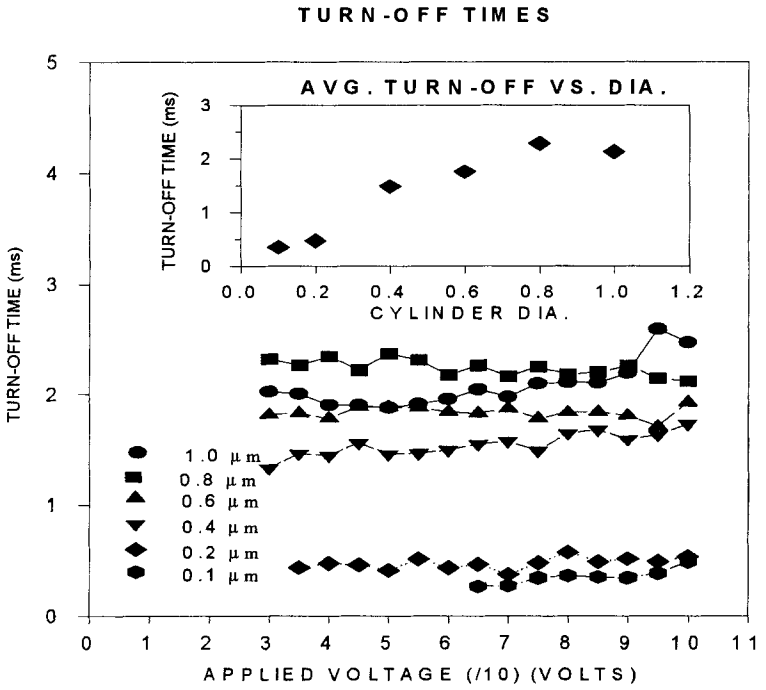

FIGURE 6 Turn-off times versus voltage for the various cylinder diameters.

turn-on time increases and then decreases with increasing voltage. A threshold effect is exhibited in which the voltage that corresponds to the maximum in the turn-on time is inversely proportional to cylinder diameter. The threshold effect is not present in cylinder sizes below 0.4 μm. At voltages below the threshold, the evolution from the zero-field to high field director configuration yields an increasing turn-on time; whereas, above the threshold voltage this evolutionary process yields turn-on times which decreases with increasing voltage. Additional evidence of this different evolutionary process from the zero-field to the nonzero-field and back to the zero-field director configurations is the sharp peak in the transmitted intensity when the voltage waveform ends (see Figure 3, 100 V_{PP}).

As shown in Figure 6, the turn-off times exhibit two regimes. For cylinder sizes equal to or greater than 0.4 μm the turn-off time is approximately 2.0 ms and for cylinder sizes less than 0.4 μm the turn-off times are on the order of 0.5 ms. The

decrease in turn-off time with cylinder size is expected because of the increased surface elastic energy contribution to the total free energy as the cylinder size decreases. For each particular cylinder size, the turn-off time is independent of voltage.

CONCLUSION

We have employed light scattering to probe the reorientation dynamics of a liquid crystal-filled porous polymer membrane. These materials exhibit novel behavior in that the turn-on time goes through a maximum and subsequently decreases as the applied voltage is increased. In addition, the turn-off times decreases as the cylinder size decreases and for cylinder sizes less than 0.4 μm the turn-off time is sub-millisecond. Presently, we are performing a theoretical analysis based on the deformation, E-field, and viscous torques utilizing the Frank free energy formalism for comparison with the experimentally measured values of turn-on and turn-off times.

ACKNOWLEDGEMENTS

The authors acknowledge the support of the National Science Foundation (NSF) under Solid-State Chemistry Grant No, DMR88-1747, the NSF Science and Technology Center ALCOM DMR89-2017, and the NSF supported Mississippi EPSCoR program. The authors also acknowledge the students who contributed greatly to the project: Mr. Demetrius McCormick, Mr. Errett Hogrefe, and Ms Kimberly Kincaid.

REFERENCES

1. J.W. Doane, N.A. Vaz, B.-G. Wu, and S. Zumer, Appl. Phys. Lett. **48**, 269 (1986).
2. J. West, Mol. Cryst. Liq. Cryst. **157**, 427 (1988).
3. Nuclepore Corporation, 7035 Commerce Circle, Pleasanton, CA 94566.
4. C.E. Williams, P.E. Cladis, and M. Kleman, Mol. Cryst. Liq. Cryst. **21**, 355 (1973).
5. M. Kuzma and M.M. Labes, Mol. Cryst. Liq. Cryst. **100**, 103 (1983).
6. S. Zumer, and J.W. Doane, Phys. Rev **1934**, 3373 (1986).
7. P.S. Drzaic, Mol. Cryst. Liq. Cryst. **154**, 289 (1988).

8. R. Ondris-Crawford, E.P. Boyko, B.G. Wagner, J.H. Erdmann, S. Zumer, J.W. Doane, J. Appl. Phys. **69** (9), 1 May 1991.
9. G.P. Crawford, M. Vilfan, J.W. Doane, I. Vilfan, I. Vilfan, Phys. Rev. A **43** (2), 1991.
10. G.P. Crawford, D.W. Allender, J.W. Doane, M. Vilfan, and I. Vilfan, Phys. Rev. A, **44** (4), 1991.
11. G.P. Crawford, D.W. Allender, J.W. Doane, Phys. Rev. A, **45** (12), 1992.